Toward microscale Cu„In,Ga…Se2 solar cells for efficient conversion and optimized material usage: Theoretical evaluation

Myriam Paire, Laurent Lombez, Jean Francois Guillemoles, Daniel Lincot

Toward microscale Cu(In,Ga)Se₂ solar cells for efficient conversion and optimized material usage: Theoretical evaluation

Myriam Paire,[a)] Laurent Lombez, Jean-François Guillemoles, and Daniel Lincot
Institute for research and development on photovoltaic energy (IRDEP), UMR 7174, EDF/CNRS/Chimie ParisTech, 6 quai Watier, 78401 Chatou, France

We develop a model to predict the performances of microscale Cu(In,Ga)Se₂ (CIGS) solar cells under concentrated sunlight, based on the study of the influence of the window spread sheet resistance, which is the first limiting factor for concentration on CIGS solar cells. This model can be used to extract the value of the sheet resistance from simple current-voltage or electroluminescence measurements. The scaling benefits associated with the operation of microscale CIGS solar cells are studied. The optimum concentration ratio, linked to the best efficiency, is calculated for different cell sizes. It is predicted that an increase from 20% efficiency, for current CIGS solar cells under 1 sun illumination, up to 30% efficiency can be expected for microscale cells under concentrated sunlight. © *2010 American Institute of Physics*. [doi:10.1063/1.3460629]

I. INTRODUCTION

With manufacturing processes cheaper than those for III-V multijunctions devices and monocrystalline silicon solar cells, while obtaining efficiencies up to 19.9%,[1] Cu(In,Ga)Se₂ (CIGS) thin film solar cells are gaining a growing market share in the photovoltaic field. CIGS thin film solar cells are mostly used under nonconcentrated sunlight, even if low concentration applications are on the way,[2,3] especially since a 21.5% efficiency under 14 suns has already been achieved.[4] In a concentrating system, the cell share can represent a third to two thirds of the module's total cost.[4,5] Drastically reducing the cell price, while maintaining its efficiency sufficiently high, is therefore a promising path for the development of concentration systems.[2] Besides, the reduction in indium or gallium consumption is a requirement for the CIGS technology, or CdTe as well, in order to scale-up at the multigigawatt level.[6–8] Developing CIGS cells for concentration is therefore a way to find optimum operating conditions, in terms of cell's efficiency and material saving.

One of the bottlenecks for the use of CIGS solar cells in a concentrating system is the limited conductivity of the transparent conducting oxide window layer. The sheet resistance of the window layer is responsible for ohmic losses that are becoming more detrimental when the cell is operated under concentrated sunlight, because of higher current densities. To overcome this difficulty, one solution is to deposit a collecting Al/Ni grid on the ZnO layer, however for high concentration ratio this may not be sufficient. Another option is to operate microscale CIGS solar cells,[9] i.e., cells which lateral dimensions are in the micrometer range. Various scaling benefits associated with the reduction in the cell size, such as increased efficiency, have already been mentioned,[5,10] but no evaluation of the gain at the microscale level for CIGS solar cells can be found. One of the main advantage of operating microscale photovoltaic cells is that

very high concentration ratio can be used, compared to current applications,[2–4] leading to higher efficiencies, as the sheet resistance effect is substantially limited. In this paper, the behavior of microscale thin film solar cells under concentration will be studied. We focus on the CIGS technology, but this study can directly be applied to other thin film technologies, such as CdTe. We develop an analytical and quantitative model to estimate the efficiency that can be expected from ultrasmall cells under concentrated sunlight. Our analysis is based on a spread sheet resistance assumption, since, especially with concentrated sunlight, the emitter sheet resistance cannot be completely described in terms of a global lumped series resistance.[11–17]

II. THE MODEL

The solar cell under study is the well-known glass/Mo/CI(G)S/CdS/ZnO cell, where the ZnO window layer has a resistivity sufficiently high to create a non negligible spread sheet resistance effect. Yet, the approach outlined here can easily be generalized to other thin film technologies. Our goal is to gain insight in the behavior of microcells under concentrated illumination.

It is generally admitted that the current-voltage (IV) relation of a solar cell can be well approximated by

$$J = J_{ph} - J_0[\exp(q(V + J \times R_s)/nkT) - 1]$$
$$- (V + J \times R_s)/R_{sh}, \qquad (1)$$

where J_{ph}, J_0 are the photocurrent and diode saturation current densities (mA/cm^2), R_s and R_{sh} the lumped series and shunt resistances ($ohm\ cm^2$), n the diode ideality factor, and kT/q the thermal voltage. The lumped series resistance approximation holds as long as the variations in the electric potential on the cell surface stay small compared to the thermal voltage kT/q. In the glass/Mo/CI(G)S/CdS/ZnO cell, the ZnO window layer is resistive enough so that this condition is not respected. This is especially true when the cell is op-

a)Electronic mail: myriam-paire@chimie-paristech.fr.

erated under concentrated sunlight. Therefore a spread sheet resistance approach is necessary.

The model proposed in this letter is based on a spread sheet resistance assumption. It is known that the results of such a model differ significantly from those of the diode model, based on Eq. (1).[13,15,16] An important advantage of considering a spread sheet resistance, is that one can analyze the scaling and geometry effects. Indeed, in Eq. (1), it is necessary to know in advance the effective series resistance of the cell, the dependence of which on the device's size is not trivial. With a distributed sheet resistance model, the input parameters are directly: the geometry of the cell (including the cell area), the resistivity, and the thickness of the layer under study. These data are easily accessible, and it is therefore straightforward to analyze the influence of the cell area or of the light concentration on the cell behavior.

The spread resistance effect is studied in the resistive window layer, of thickness t. For the sake of simplicity, we made several assumptions, which do not limit the extent of the study. The resistivity and thickness of the window layer as well as the illumination are taken constant over the cell. Therefore, the photocurrent J_{ph} and the diode saturation current J_0 are considered uniform for a given illumination. The cell is considered circular of radius a, and the current is supposed to be horizontal in the window layer. As we do not consider leakage currents, the current entering in the layer from the p-n junction is equal to the current collected at the electrode, according to Kirchhoff's laws. When operated under concentrated sunlight J_{ph} becomes $J_{ph}(1 \text{ sun})^*C$, where C is the concentration ratio.

The equations we use to describe the problem are well known[17,18] and we recall them for the sake of clarity. The window layer is considered resistive in the sense of Ohm's law, that is

$$\vec{J} = -1/\rho \; \text{grad}(\psi), \qquad (2)$$

where J is the current density, ρ the window layer's resistivity, and ψ the electric potential.

In the absence of fixed charges in the ZnO layer, from Gauss's law follows:

$$\text{div}(\vec{J}) = 0. \qquad (3)$$

The current density coming from the p-n junction is supposed to be

$$J_z(z=0) = J_{ph} - J_0\{\exp[q\psi(z=0)/nkT] - 1\}$$
$$- \psi(z=0)/R_{sh}, \qquad (4)$$

where ψ is the electric potential in the window layer and z the altitude, which is set to 0 at the bottom of the window layer and equals t at the surface, J_{ph}, J_0, n, kT/q, R_{sh} are, respectively, the photocurrent density, the diode saturation current density, the diode ideality factor, the thermal voltage, and the shunt resistance. The series resistance of the junction itself is neglected, its influence being incidental compared to the spread sheet resistance. The shunt resistance can also be neglected, as in the case of very efficient solar cells the values of the shunt resistance are very high. Unless otherwise told, R_{sh} is taken infinite in our calculations. Because of the circular symmetry of the cell, the potential ψ and the current densities J only have a radial component. We also consider that the window layer thickness t is much smaller than the cell radius a (in CIGS solar cells, the thickness t of the window layer is approximately 400 nm). Therefore, we define electric potentials and currents that have no z-dependence by estimating an average value with respect to the thickness. For instance, we define the average current density in the horizontal plane $\vec{J}_\parallel$ as

$$\vec{J}_\parallel(x,y) = 1/t \int_0^t \vec{J}_{horiz}(x,y,z)dz, \qquad (5)$$

where $\vec{J}_{horiz}$ refers to the current density in the horizontal plane and t is the thickness of the window layer. If we integrate Eq. (3) with respect to the thickness of the film, we obtain

$$1/t \int_0^t \text{div}(\vec{J})dz = 0,$$

$$\Rightarrow \text{div}(\vec{J}_\parallel) + 1/t \; \text{div}\left(\int_0^t \vec{J}_z dz\right) = 0,$$

$$\Rightarrow \text{div}(\vec{J}_\parallel) + [J_z(z=t) - J_z(z=0)]/t = 0, \qquad (6)$$

where $\vec{J}_z$ refers to the current density along the z-direction, and J_z to its norm. We estimate that $J_z(z=t)=0$. We choose the cylindrical coordinates (r,θ) to describe our problem and we fix the origin at the cell's center. Because of the circular symmetry of the cell the electric potential and the current density, that are radial, are also considered to have no dependence on the θ coordinate. Combining Eqs. (2)–(4) and (6), the potential ψ on the surface of the cell is the solution of the following one-dimensional equation:

$$\partial^2\psi/\partial r^2 + 1/r \times \partial\psi/\partial r + R_\square\{J_{ph} - J_0[\exp(q\psi/nkT) - 1]\}$$
$$- \psi/R_{sh} = 0, \qquad (7)$$

where $R_\square = \rho/t$ is the sheet resistance (ohm/square) and ρ the resistivity of the window layer.

In order to solve this equation, appropriate boundary conditions are needed. The first boundary condition is that at the electric contact between the window layer and the external circuit, the potential ψ equals the applied potential V. The second condition depends on the geometry. In this paper, we consider two different geometries. First we consider that the electric contact on the window layer is taken with a probe of radius b, placed at the center of the cell of radius a. Therefore, the probe perimeter is an equipotential at the applied voltage V, $\psi(b)=V$ and in the absence of surface charge or recombination at the cell perimeter, we have the Neumann condition $\partial\psi/\partial r(a)=0$. This contact geometry will be designated by dot contact (DC). Second, we considered the case where the contact is taken by the deposition of an annular electrode at the periphery of the cell (designated as ring contact or RC). In this case, $\psi(a)=V$, and due to the circular symmetry there is no net current at the center of the cell, i.e., $\partial\psi/\partial r(0)=0$.
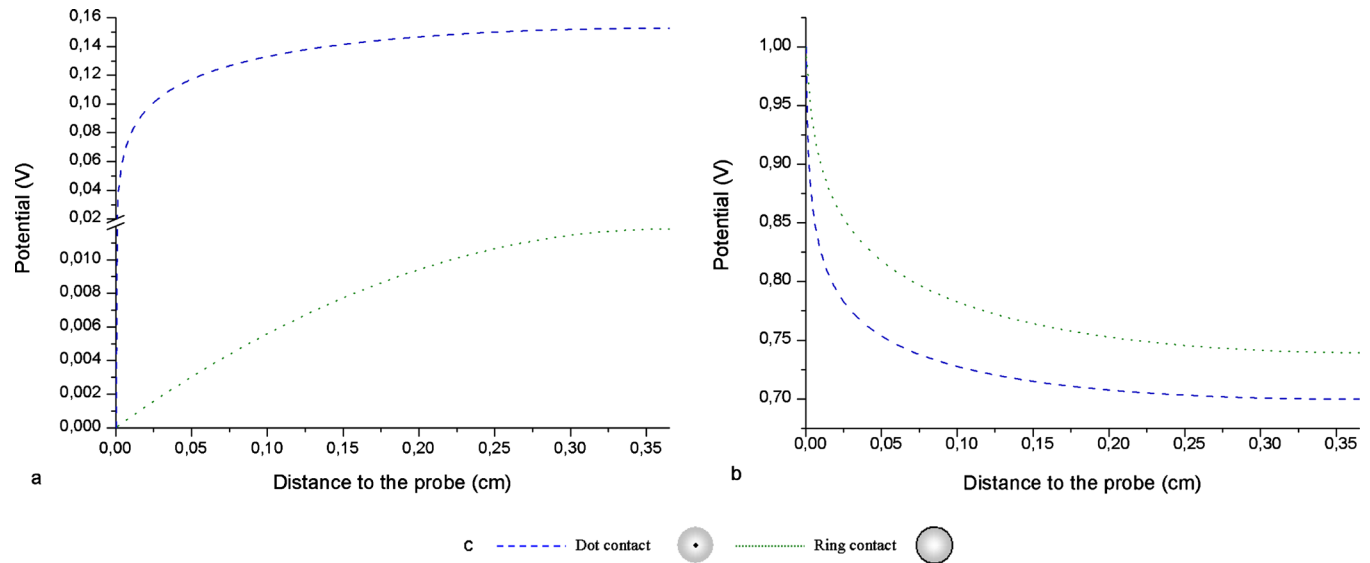
FIG. 1. (Color online) Potential ψ vs the distance to the probe (area 0.419 cm^2_$R_\square$=10 ohm/square) for the DC (blue string line) and RC (green dot line). The operating point are open circuit under illumination (a) and V=1 V in the dark (b). The legend and a scheme of each contacting geometry is displayed in (c).

The system of Eq. (7) and its boundaries conditions is not solvable analytically. With a standard solver software, we obtain a numerical solution for chosen parameter values. The inputs of our calculations are the diode characteristics of the record National Renewable Energy Laboratory (NREL) solar cell[1] (area 0.419 cm^2, n=1.14, J_0=2.1×10^{-9} mA/cm^2, J_{sc} =35.5 mA/cm^2). We assumed a ZnO sheet resistance of 10 ohm/square and in the case of a probe contact we consider a probe of radius 3.5 μm.

Our model is based on known equations and other groups are also interested in the influence of the window layer sheet resistance,[14] but yet the object under study in this paper is entirely new. As far as the authors know, there is currently no study of the potential of microscale CIGS cells for concentration. The following results are, therefore, a guideline for the development of such high efficient solar cells.

III. RESULTS

The resolution of Eq. (7) enables us to gain access to the repartition of the potential and the current density in the window layer.

Figure 1 displays the potential as a function of the radial distance for the dot and ring contact geometry for two different configurations: open circuit under 1 sun and 1 V under dark conditions. We can clearly see that the potential is not constant over the cell area. The variation in the potential is greater than kT/q (25.8 mV), thus confirming that a lumped resistance analysis is not valid, even for low window layer sheet resistance ($R_\square$=10 ohm/square). In the case of the open circuit under illumination, the current density, proportional to the derivative of the potential, is predominantly concentrated around the electrode probe for the DC geometry, which is something that has already been observed.[14] For the RC, however, the larger contacting perimeter leads to a current density that is much less concentrated in the vicin-

ity of the probe. We expect that the RC geometry will yield better cell performances, as a homogeneous repartition of current density over the cell diminishes the spread sheet resistance effects. It is therefore crucial to develop appropriate contacting geometries for microscale solar cells, in order to diminish as much as possible the sheet resistance losses and to take full advantage of the scaling benefits.

For the dark condition under an applied voltage of 1 V, we can see that there is a voltage drop when we go further from the electrode. This can simply be assessed by an electroluminescence (EL) experiment.

EL experiments are already used as quality tests of single solar cells or modules, in order to detect series and shunt resistance problem that may have occurred in the fabrication processes.[19–21] As one of these authors suggested,[19] it is indeed possible to extract the value of the window layer sheet resistance from an EL experiment. Under dark conditions, we apply a voltage to the surface of a standard CIGS solar cell (0.1 cm^2) with a tungsten probe, linked to a Keithley 2635A source meter. We detect the luminescence with a charge coupled device camera mounted on a microscope, thus enabling to visualize the repartition of the luminescence on the cell [Fig. 2(a)]. The luminescence profile [Fig. 2(b)] is determined by integrating the intensity detected over a 180° angular sector centered at the probe tip. The luminescence is normalized by dividing the luminescence signal by its maximum value. In order to know exactly the potential applied to the ZnO layer, one must know the resistance associated with the probe/ZnO contact. We determined it by studying the luminescence signal at different potentials, and we deduced that the applied potential was 0.71 V. The luminescence intensity Φ is supposed to be related to the voltage V between the back contact and the ZnO by

$$\Phi = \Phi_0 \exp(qV/kT), \tag{8}$$

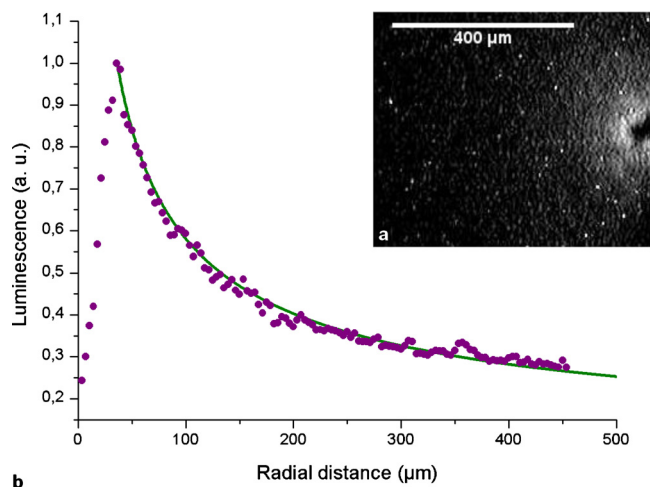where kT/q is the thermal voltage and Φ_0 a calibration factor that depends on the camera settings.

FIG. 2. (Color online) (a) EL image of a 0.1 cm² CIGS solar cell, contacted by a tungsten probe under an applied voltage of 0.71 V. (b) Integrated luminescence intensity vs radial distance from the probe: the dots correspond to experimental data—the green line is our model's simulation.

It is clear that the intensity of the luminescence decreases with the distance to the electrode, thus confirming a voltage drop on the surface (the first 50 μm are relatively dark because of the shading due to the probe). We fit the EL signal by our model, in order to determine the sheet resistance that leads to such a luminescence decay with radial distance. We simulate the potential repartition with the radial distance for a model cell, and we deduce the expected luminescence with Eq. (8). We adjust the sheet resistance parameter in order to obtain the best fit. For the experiment of Fig. 2, we found $R_\square = 30 \pm 1$ ohm/square, which was the expected value. Therefore, we prove that this EL experiment is a way to gain access to a local sheet resistance value very easily.

We have determined the repartition of the potential on a cell surface and assessed the results with an EL experiment. Once the electric potential and the current density estimated over the cell area for a given applied voltage V, it is straightforward to deduce a current-potential curve.
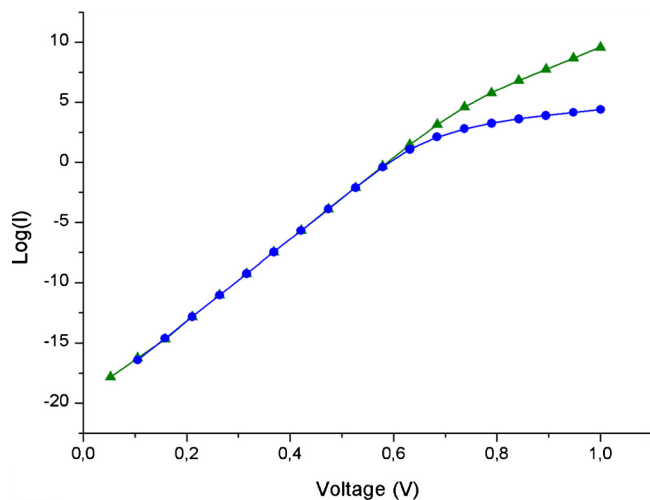

FIG. 3. (Color online) Log(|J|) vs voltage. Triangles correspond to the RC geometry, dots to the DC geometry.
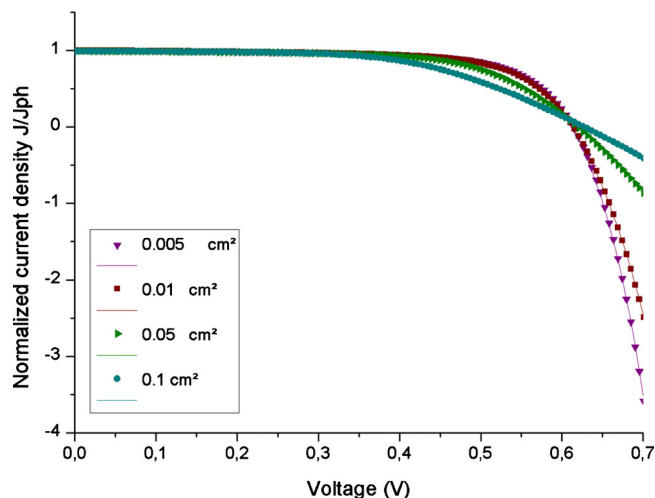

FIG. 4. (Color online) Normalized IV curves J/J_{ph} vs voltage (V). Lines represent the experimental data, and the dots are the simulation results.

Figure 3 shows a log(|J|)=f(V) curve for a 0.419 cm² cell in dark conditions, with the diode characteristics of the record NREL cell, and a sheet resistance of 10 ohm/square, for both the dot and ring contact geometries. Once again we can clearly see the influence of the contact geometry: for the same cell, with the same sheet resistance, if a RC is employed the resistive losses are less detrimental than with the DC, which can be seen from a steeper incline of the log(J) curve at high potentials. This confirms that much attention has to be paid to the contact engineering for ultrasmall cells.

Once the current-potential curve calculated, it is possible to estimate the efficiency, open circuit voltage, short circuit current density, fill factor (FF) of a given solar cell under a certain illumination. The role of cell size, sheet resistance and light concentration can be analyzed. We first studied the role of the cell size under one-sun illumination. We study cells of four different areas: 0.1, 0.05, 0.01, and 0.005 cm². The cells are obtained by mechanical scribing on the same Glass/Mo/CIGS/CdS/iZnO/Al:ZnO stack, and the cell area is defined with a 3% uncertainty. The scribed cells are square; in our calculations they are modeled by circular cells of the same area, i.e., with radius of 1780 μm, 1260 μm, 560 μm, and 400 μm, respectively. The CIGS film is provided by the Zentrum für Sonnenenergie-und Wasserstoff-Forschung (ZSW), the chemical bath deposition deposited CdS film and the sputtered ZnO layers are deposited in our laboratory. We measure the IV curve under one sun, using a AM1.5 solar simulator. The cells are contacted by a tungsten probe at their center and no collecting grid is deposited. This contacting method is associated with a certain contacting resistance. In our case, considering the tungsten probe and the ZnO surface, we evaluate this contact resistance to 10 ohms, and take it into account separately from the sheet resistance. We use a diode-fit to extract the diode parameters of the cells, and we use our model to evaluate the sheet resistance, with help of a nonlinear least-square fit (Fig. 4). We analyzed three cells of each size and we found that the sheet resistance is approximately the same among the different cells, the sheet resistance being on average 31 ohm/square

TABLE I. Average sheet resistance resulting of a fit of IV measurements.

Cell radius (μm)	1780	1260	560	400
Estimated sheet resistance (ohm/square)	34 ± 2	30 ± 1	31 ± 6	29 ± 3

(± 2 ohm/square) (Table I). This is what is expected, since the cells are scribed on the same substrate.

In Fig. 4, the decrease in the FF in bigger cells, corresponding to more important resistive losses, is therefore a cell size's effect only and is not associated with an increase in the window layer resistivity. In Fig. 4, we plot IV curves for the experimental and the corresponding simulated data: the current density is normalized by the photocurrent, thus the shading, that is more detrimental for small cells since the same probe is used for all measurements, is not taken into account. We can see that in small cells the resistive effect is less detrimental, resulting in higher FF. Thus, we can consider operating microscale cells under concentrated light, because up to a certain concentration ratio, the resistive losses will not be a limiting factor. From this point, we need to study which concentration ratio will be optimum for a given cell, and which efficiencies can be expected. Our model, which is proved to be efficient in analyzing experimental data, will be used to predict the behavior of microscale solar cells.

We study the variation in the efficiencies with concentration ratio of four different cells: 10^{-1} cm², 10^{-2} cm², 10^{-3} cm², and 10^{-5} cm² (1780 μm, 564 μm, 178 μm and 18 μm of radius, respectively) for a DC [Fig. 5(a)]. The concentration ratio is defined as the ratio of the incident light power density by light power density at 1 sun (100 mW/cm²). Up to a certain incident light power, or a certain concentration ratio for a given cell area, the performances of the cell are improved by concentration (the efficiency is proportional to the logarithm of concentration, as

expected with this model), until a point where the Ohmic losses induced by the sheet resistance are important enough to deteriorate the cell performance. It is therefore possible to estimate for a certain cell, its optimum working conditions and the corresponding efficiency. Figure 5(a) shows that the best use of the incoming power is made by small cells under concentrated sunlight. For example, for an incident power of 1×10^{-2} W, that is for the total power collected at 1 sun by a surface of 10^{-1} cm², the 10^{-1} cm² solar cell will yield a 19.4% efficiency, the 10^{-2} cm² solar cell (operated under 10 sun) a 22% efficiency, the 10^{-3} cm² solar cell (operated under 100 sun) a 24% efficiency, and the 10^{-5} cm² cell operated under 30 000 sun is 30% efficient. One can notice that the maximum efficiency for each cell occurs to a first approximation for the same total incident light power. This can be explained by a simple adimensional analysis of Eq. (7). The adimensional equivalent of Eq. (7) is

$$\partial^2 v/\partial R^2 + 1/R \times \partial v/\partial R + \alpha\{1 - j_0[\exp(v) - 1]\} = 0, \quad (9)$$

where the adimensional variables are $\alpha = R_\square \times a^2 \times C \times J_{ph}(1 \text{ sun}) \times q/nkT$, $j_0 = J_0/[C \times J_{ph}(1 \text{ sun})]$, $j_{ph} = 1$, $R = r/a$ and $v = q\psi/nkT$. If the incident light power is constant, so is the product $a^2 \times C \times J_{ph}(1 \text{ sun})$, and therefore the variable α, as well as v and R, is unchanged. Thus, we can expect at the first order that the maximum efficiency occurs for the same value of the incident light power, and it is what we observe on Fig. 5. The deviation one can note for high concentration ratios is due to the dependence of the adimensional variable j_0 on concentration.

One can notice that for ultrasmall cells, the sheet resistance value is not a limiting factor for the cell efficiency. In Fig. 5(b), we study the efficiencies of a cell of radius 18 μm of increasing sheet resistance (10–100–1000 ohm/square) with concentration ratio for a RC. We see that for the cell with a sheet resistance of 10 or 100 ohm/square, the resistance is hardly a limiting factor, and for the cell with sheet resistance of 1000 ohm/square, the concentration is interest-
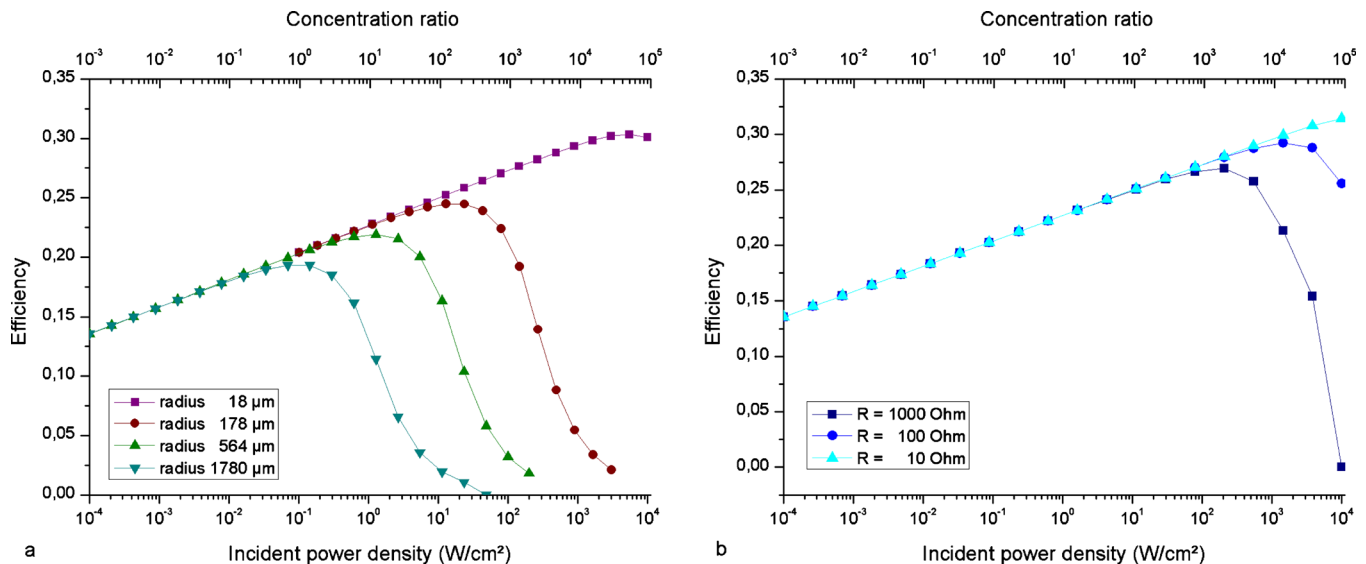

FIG. 5. (Color online) (a) Efficiency vs concentration ratio for three cells: radius 1784 μm (10^{-1} cm²), 564 μm (10^{-2} cm²), 178 μm (10^{-3} cm²), and 18 μm (10^{-5} cm²), DC geometry, sheet resistance of 10 ohm/square. (b) Efficiency vs concentration ratio for a cell of radius 18 μm (10^{-5} cm²), for three different sheet resistances 10, 100, and 1000 ohm/square, RC geometry.
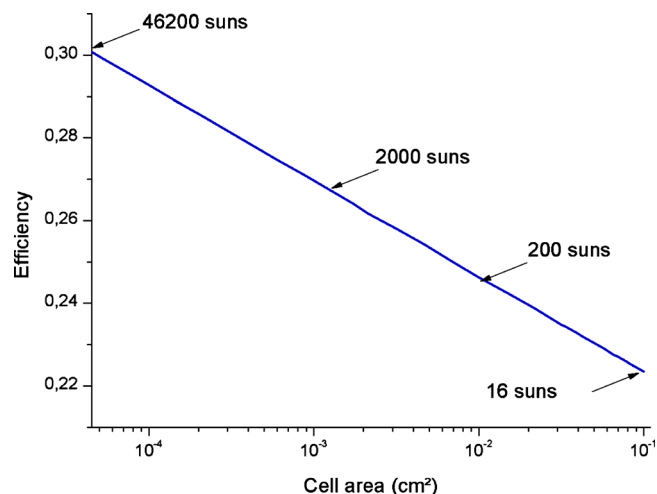
FIG. 6. (Color online) Efficiency vs cell area (cm^2) in the RC geometry, $R_\square=10$ ohm/square. Four concentration ratios are given for information.

ing until 5000 sun. Therefore, the sheet resistance is no longer the first optimization parameter in the window layer. As the constraint on the sheet resistance of the ZnO layer is loosen, one can optimize the transparency, by using a thinner window layer for example. The advantages associated with microscale solar cells are not only that one can reach higher efficiencies with concentration because of limited resistive losses, but also that higher photocurrent can be expected as the transparency of the window layer can be improved.

We prove that it is preferable to concentrate light on small cells rather than using large cells under one sun illumination, from an electrical point of view. The optimum concentration ratio for a given cell size is dependant on the sheet resistance, cell diode characteristics but also on surface recombination losses, especially side recombination losses,[5] cost of concentrating optics, the latter not being taken into account in our simulations. A study of thermal losses associated with high concentration ratio should also be made to complete our study. Yet, it is expected that for microscale cells the thermal losses will not be a limiting factor.[10] As some of the above parameters are not clearly determined for microscale CIGS solar cell, experimentation and further fundamental knowledge are needed for a more precise analysis. However, our results show undoubtedly that there is a regime where sheet resistance is not a limiting factor for microscale CIGS solar cells under concentrated sunlight, allowing very high efficiencies of CIGS solar cells for a limited cell price.

One important point is to determine the optimum operating point and the corresponding efficiency for a given cell. Figure 6 displays the maximum efficiency expected for a given cell area, calculated as the efficiency observed for the optimum concentration ratio. For information, we show the corresponding optimum concentration ratio for certain cell sizes $(10^{-1}-10^{-2}-10^{-3}-4.5\times10^{-5}$ cm$^2)$. For cells which sizes are smaller than 4.5×10^{-5} cm^2, the optimum concentration ratio found in our calculations exceeds the limit concentration of 46 200, indicating that the spread sheet resistance is no longer a limiting factor for the cell performance (the efficiencies for smaller cells, with optimum concentration higher than 46 200, are irrelevant and not displayed on

this graph). As expected, the RC method yields higher efficiency than the dot one for a given size, as the spread sheet resistance effect is diminished. A 10^{-1} cm^2 solar cell (operated under 16 sun) will yield a 22% efficiency, the 10^{-2} cm^2 solar cell (operated under 200 sun) a 24% efficiency, the 10^{-3} cm^2 solar cell (operated under 2000 sun) a 27% efficiency and a 10^{-5} cm^2 solar cell (of radius 18 μm) operated at 46 200 sun yields 31% efficiency but higher efficiency could be expected at even higher concentration ratios.

IV. SUMMARY

We developed a theoretical approach to predict the potential of microscale CIGS solar cell. Our model, based on spread sheet resistance, has proven to be a useful tool to analyze experimental data, such as IV curves or EL studies. We found that very important scaling benefits, associated with the decrease in cell area from the current centimeter square range to a micron square range, are to be expected, especially in terms of efficiency, but also in terms of material consumption. It was predicted that the CIGS technology, which yields nearly 20% efficiency at 1 sun for cells in the centimeter square range, can yield up to 30% efficiency under concentrated sunlight in the micron square range, while conserving the stacking architecture and materials properties. We also pointed out the importance of the contact geometry. As our approach is not limited to the CIGS technology, similar efficiency gains associated to microscale cells can be expected from other thin film technologies.

ACKNOWLEDGMENTS

[1]I. Repins, M. A. Contreras, B. Egaas, C. DeHart, J. Scharf, C. L. Perkins, B. To, and R. Noufi, Prog. Photovoltaics **16**, 235 (2008).
[2]J. R. Tuttle, A. Szalaj, and K. Beninga, Conference Record of the 28th IEEE Photovoltaic Specialists Conference, Anchorage, Alaska, 15–22 September 2000, pp. 1468–1471.
[3]J. Wennerberg, J. Kessler, J. Hedstrom, L. Stolt, B. Karlsson, and M. Ronnelid, Sol. Energy **69**, 243 (2001).
[4]J. S. Ward, K. Ramanathan, F. S. Hasoon, T. J. Coutts, J. Keane, M. A. Contreras, T. Moriarty, and R. Noufi, Prog. Photovoltaics **10**, 41 (2002).
[5]C. Algora, I. Rey-Stolle, B. Galiana, J. R. Gonzalez, M. Baudrit, and I. Garcia, Conference Record of the 2006 IEEE 4th World Conference on Photovoltaic Energy Conversion, Waikoaa, Hawaii, 2006, ISBN: 1-4244-0017-1, Vols. 1 and 2, pp. 741–744.
[6]A. Feltrin and A. Freundlich, Renewable Energy **33**, 180 (2008).
[7]V. Fthenakis, Renewable Sustainable Energy Rev. **13**, 2746 (2009).
[8]B. A. Andersson, Prog. Photovoltaics **8**, 61 (2000).
[9]Patent pending.
[10]G. N. Nielson, M. Okandan, P. J. Resnick, J. L. Cruz-Campa, P. Clews, M. Wanlass, W. Sweatt, E. Steenberger, and V. P. Gupta, 24th European Photovoltaic Solar Energy Conference, Hamburg, Germany, 21–25 September 2009, edited by W. Sinke, H. Ossenbrick, and P. Helm, WIP-Renewable energies, ISBN: 3-936338-25-6, pp. 170–174.
[11]A. de Vos, Sol. Cells **12**, 311 (1984).
[12]B. Galiana, C. Algora, and I. Rey-Stolle, Sol. Energy Mater. Sol. Cells **90**, 2589 (2006).
[13]G. T. Koishiyev and J. R. Sites, Sol. Energy Mater. Sol. Cells **93**, 350 (2009).
[14]U. Malm and M. Edoff, Prog. Photovoltaics **16**, 113 (2008).

[15]L. D. Nielsen, IEEE Trans. Electron Devices **29**, 821 (1982).

[16]G. M. Smirnov and J. E. Mahan, Solid-State Electron. **23**, 1055 (1980).

[17]N. C. Wyeth, Solid-State Electron. **20**, 629 (1977).

[18]A. S. H. van der Heide, A. Schonecker, J. H. Bultman, and W. C. Sinke, Prog. Photovoltaics **13**, 3 (2005).

[19]A. Helbig, T. Kirschartz, R. Schaeffler, J. Werner, and U. Rau, 24th European Photovoltaic Solar Energy Conference, Hamburg, Germany, 21–25 September 2009, edited by W. Sinke, H. Ossenbrick, and P. Helm, WIP-Renewable energies, ISBN: 3-936338-25-6, pp. 2446–2449.

[20]H. Sugimoto, T. Aramoto, Y. Kawaguchi, Y. Chiba, S. Kijima, Y. Fujiwara, Y. Tanaka, H. Hakuma, K. Kakegawa, and K. Kushiya, 24th European Photovoltaic Solar Energy Conference, Hamburg, Germany, 21–25 September 2009, edited by W. Sinke, H. Ossenbrick, and P. Helm, WIP-Renewable energies, ISBN: 3-936338-25-6, pp. 2465–2468.

[21]T. Weber and M. Kutzer, 24th European Photovoltaic Solar Energy Conference, Hamburg, Germany, 21–25 September 2009, edited by W. Sinke, H. Ossenbrick, and P. Helm, WIP-Renewable energies, ISBN: 3-936338-25-6, pp. 477–479.